

CW ND:YAG LASER WELDING OF DISSIMILAR SHEET METALS

Paper # 803

M. Theron, C. van Rooyen, L.H. Ivanchev

National Laser Centre, CSIR
Meiring Naude Rd, Pretoria, 0001, South-Africa

Abstract

A 4kW CW Nd:YAG laser was used for lap welding of three different dissimilar sheet metal combinations, namely 316L S/S - Ti64, 316L S/S - Al 5052 and Al 1200 - Cu (99.85%). A welding matrix of laser power, travel speed and spot sizes was investigated in order to determine the operating windows for the specific set-up.

Sound lap welds could be obtained with the Al/Cu and SS/Al dissimilar combinations, but only within narrow operating windows. Extremely hard phases were obtained within the fusion zones, especially in the SS/Ti welds, resulting in very brittle welds which were prone to cracking.

Key-words: Dissimilar lap welding, welding matrix, operating windows

Introduction

In recent times there has been an increased interest in the use of welding techniques to join dissimilar materials.

The material combination Al/Cu is a combination of generally different materials that finds particular use in electronic and electrical applications. Pure aluminum has little strength, but possesses high electrical conductivity, reflectivity and corrosion resistance. Compared to Cu, aluminum has, however, a slightly smaller thermal and electrical conductivity, but it is large enough for a wide range of applications[1,2]. Next to steel, aluminum is the most commonly used and commercially available metal due to its light weight and high strength-to-weight ratio and the stainless steel/aluminum combination nowadays also has applications in small ship/yacht-building[3]. The stainless steel/titanium combination has applications in the medical industry[4].

During laser welding, mainly two groups of material characteristics have an influence on the results and could lead to problems, namely physical- and metallurgical characteristics. Physical characteristics such as absorption at the laser wavelength and heat

conductivity strongly influence the melting process and the thermodynamics. Poor absorption at the laser wavelength, high heat conductivity (as is the case with Al and Cu) and insufficient viscosity of the fused material typically result in a narrow process window between sufficient fusion and excessive penetration, excessive spatter and limitations on reproducibility[1,5].

Metallurgical characteristics of the two constituents of the dissimilar combination determine the characteristics of the fusion zone which includes possible hardening mechanisms. These in turn influence the mechanical and functional characteristics of the welded joint. Low-melting point, high volatility alloying elements introduce instability in the welding process which together with the presence of insoluble alloy components and precipitation of brittle phases often limit the mechanical strength of the joint[1,6].

For many material combinations, the formation of particular intermetallic phases in the fusion zone gives rise to major problems. These situations can occur because of the lack of solubility (metallurgical affinity) of the material components and are often characterized by high hardness and brittleness[1,3].

In addition to the formation of brittle aluminum-rich intermetallic compounds, the other main challenge presented by the fusion welding of aluminum to steel results from the large difference in melting temperatures. The technique of melting one metal by heat conduction is not applicable to SS and Ti, due to similar thermo-physical properties. To produce a metallurgical bonding, both metals have to be molten. Furthermore, the difference in the thermal expansion coefficient is large, which leads to stress in the joint interface[4,7].

For good weld joint strength involving combinations of dissimilar metals, the formation of a solid solution in the weld pool is needed and not the formation of intermetallics. It is, therefore, critical to minimize the thickness of intermetallic phases in the fusion zone[1,3,5,8].

Experimental procedure

Lap welding of three different dissimilar metal combinations was investigated, namely 316L S/S - Ti64, 316L S/S - Al 5052 and Al 1200 - Cu (99.85%). All sheet materials were 0.9mm thick, except the titanium which was 0.8mm thick.

In the case of the SS-Ti64 and SS-Al combinations, the stainless steel sheet was welded on top of the other two materials, whereas with the Al-Cu, the aluminum was on top. In the first-mentioned case, SS was welded on top in order to avoid additional shielding required with Ti and in the latter case, no BOP could be performed on the Cu due to insufficient power density available from the specific Nd:YAG laser.

Experimental Set-Up

A Precitec YW50 welding head coupled to a 6-axes KUKA KR60L30HA articulated arm robot was used with a 4kW CW Nd:YAG laser which was delivered through a 400 micron fibre. A 200 mm collimator was used with 150mm, 200mm and 300mm FL lenses in order to produce three different spot sizes. The incident beam was perpendicular for SS (Fig. 1) and at a drag angle of 15° for Al. The sheet metal samples were clamped in an overlap configuration with a specially made jig in order to eliminate any gaps between the sheets. He @ 10 l/min was applied as shielding gas via a co-axial nozzle (with the 150 and 200mm lenses) and a 4.5mm Ø off-axis nozzle (with the 300mm lens). The lap welds were performed with the focal plane either at the top surface of the top plate or 1mm below the top surface in some cases.

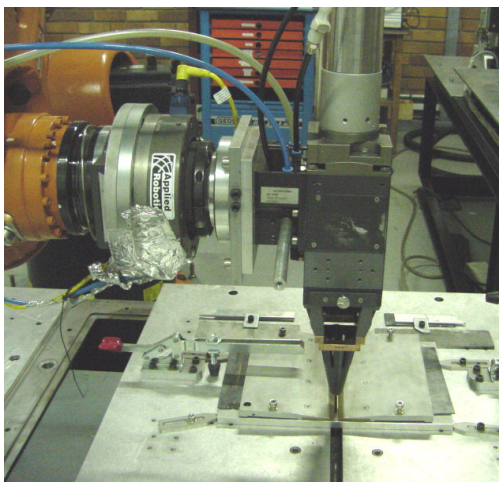


Figure 1: Example of experimental set-up for S/S-Al and S/S-Ti64 dissimilar lap welding

All aluminium and titanium surfaces were wire-brushed prior to welding to remove the oxide layer, and cleaned with acetone, whereas the stainless steel and copper surfaces were only cleaned with acetone.

Experimental Parameters

A welding matrix of spot size, laser power and travel speed was investigated. For each spot size the power was varied in discrete steps over a power range that was determined as follows: The lower power limit was determined by the power required for full penetration of the top sheet in the lap configuration. The upper power limit was determined by limitations in the available travel speed, immediate cracking or start of full penetration through both metal sheets.

Due to the above, the power density range investigated for the aluminum/copper combination varied between 13 and 32 kW/mm² and the travel speed between 1.5 and 7 m/min (HI=19-62 J/mm). For the stainless steel/aluminum combination it varied between 3 and 19 kW/mm² and 1.5 – 6 m/min (HI=11-36 J/mm). Lastly, for the stainless steel/titanium combination it ranged between 6 and 19 kW/mm² and 4.5 – 9 m/min (HI=6-19 J/mm).

Microstructural Investigation And Mechanical Testing

The welded samples were studied and evaluated by means of X-rays, stereo and optical microscopy, SEM analyses coupled with EDX, micro-hardness testing as well as tensile shear testing. General, as well as specific chemical analyses were made within the welds in order to try and identify the phases present and to correlate the analyses with the hardness in those areas.

Tensile-shear testing was done on all the lap welds. The specimens were prepared by means of water-jet cutting. Specimen sizes complied with the AWS C1.1 specification: Recommended Practice for Testing Resistance Welds. The parameter sets which yielded the best tensile shear strengths were then further investigated and tested, except for the SS/Ti combination.

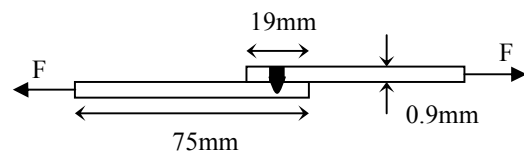


Figure 2: Tensile shear specimen size of the dissimilar lap welds, and direction of tension

Results and discussion

Microhardness

Vickers micro-hardness traverses were done through the centre of the welds (from root to weld surface) and the results obtained over the investigated power density ranges, are given in Figure 3. The Vickers hardness of the base materials were Cu = 83, Al 1200 = 28, SS = 200, Al 5052 = 75 and Ti64 = 335 HV_{0.3}.

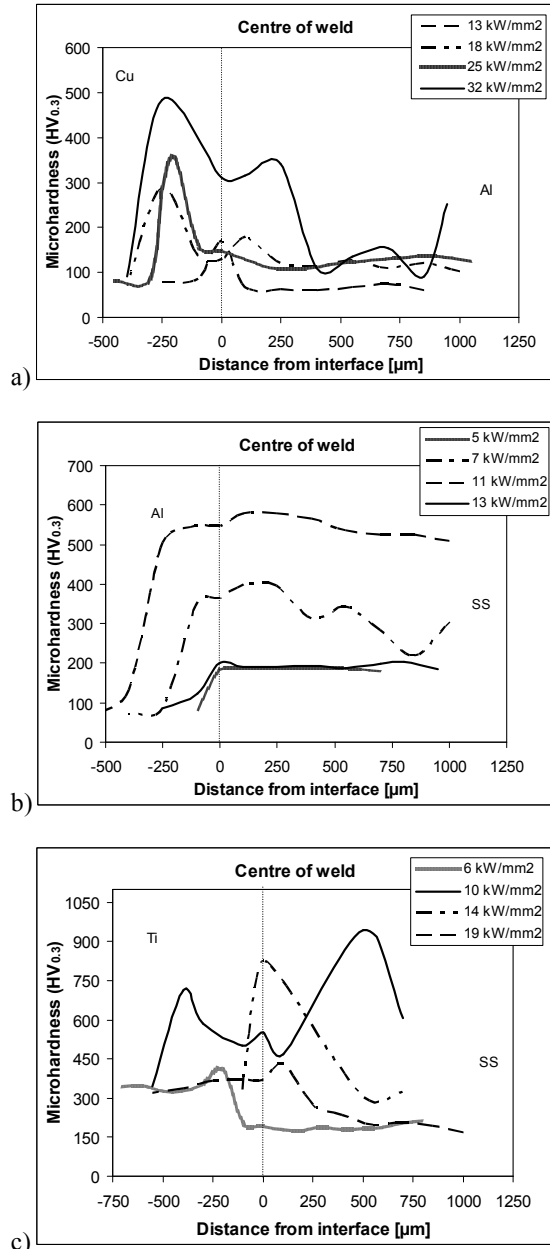


Figure 3: Microhardness traverses (root to surface) for a) Al/Cu b) SS/Al and c) SS/Ti lap welds

The centre-weld microhardness in the fusion zone (weld metal just above the fusion line) increases with increasing power density (decreasing heat input) for all three dissimilar metal combinations (Fig.3). However, it seems that the hardness then decreases again for SS/Al and SS/Ti above 11 kW/mm² and 14 kW/mm² respectively. This might be attributed to the smaller dilution obtained at the specific welding parameters (Fig. 12).

In general, the hardness within the weld metal (away from fusion line) does not vary much for all three dissimilar metal combinations, with the exception of one or two lap welds. For the Al/Cu and SS/Ti, most of the welds show the highest hardness in the fusion zone and decreasing hardness towards the rest of the weld metal. However, for SS/Al, the hardness mostly increases over the fusion zone up to the hardness of the weld metal away from the fusion line.

The hardness traverses reflect mostly the variations in chemical composition within the welds found by means of EDX analyses (Fig. 7).

The high hardness in the fusion zones might be attributed mainly to the formation of intermetallic phases, but to some extent also to the very fine microstructure resulting from very high cooling rates during laser welding and super saturated solid solution of Cu in Al, Al in Fe and Ti in Fe.

Microstructures And SEM Analyses

Figures 4 – 6 show the optical and SEM microstructures, EDX spectra images and analyses for some lap welds of all three dissimilar combinations.

It is evident that convection is dominant in metal transfer in the Al/Cu and SS/Ti welds, but not in the SS/Al welds, because a very homogenous chemical composition can be observed for the SS/Al in Figure 5, with only low percentage of Al in the weld metal away from the fusion zone.

From Figure 4 it can be seen that in some areas of the weld fusion zone the Cu only melted and recrystallised and it seems that only a thin layer (<10μm) of an intermetallic compound developed. The intermetallic was however not identified.

Figure 5 indicates the presence of solute bands in the fusion zone (optical micrograph) as well as the possible presence of Fe₂Al (EDX analysis), but this was not confirmed. The HAZ in the Al adjacent to the fusion line, can clearly be seen due to the dendritic structure present.

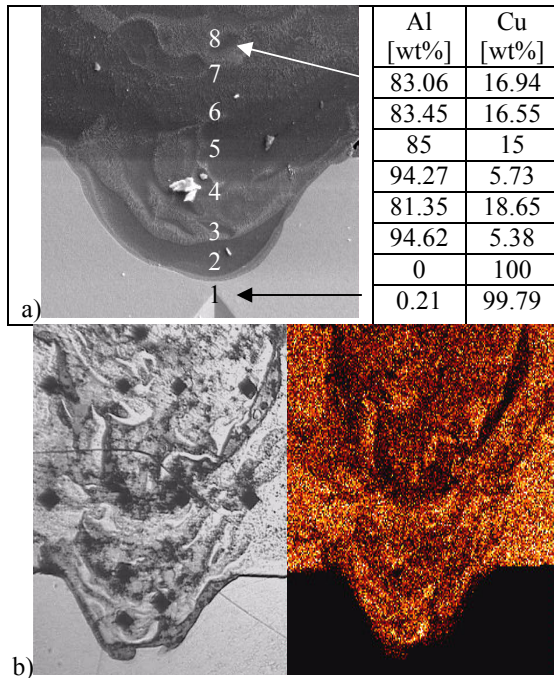
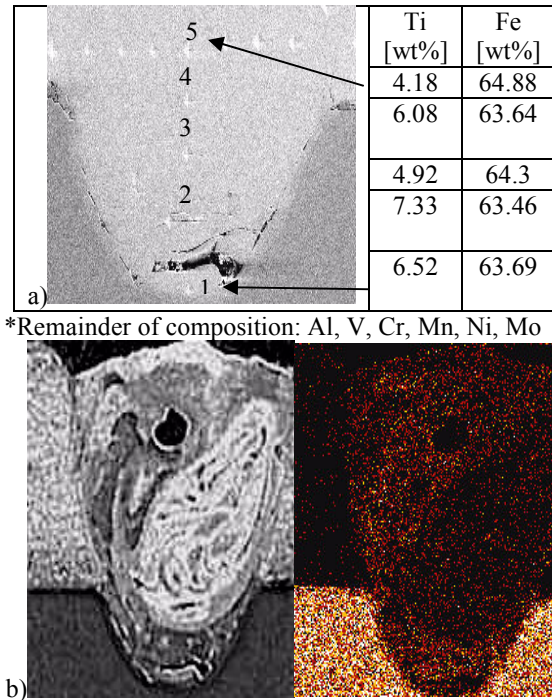
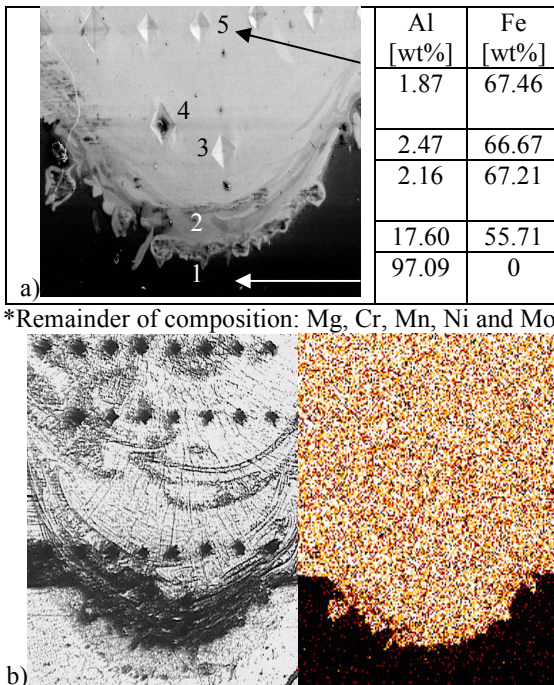


Figure 4: a) EDX analyses across the fusion line and b) Optical microstructure and EDX spectra map image for Al, of the Al-Cu lap weld done at 19 kW/mm² (HI = 32 J/mm)



*Remainder of composition: Al, V, Cr, Mn, Ni, Mo

Figure 6: a) EDX analyses across the fusion line and b) Optical microstructure and EDX spectra map image for Ti, of the SS-Ti lap weld done at 10 kW/mm² (HI = 23 J/mm)



*Remainder of composition: Mg, Cr, Mn, Ni and Mo

Figure 5: a) EDX analyses across the fusion line and b) Optical microstructure and EDX spectra map image for Fe, of the SS-Al lap weld done at 13 kW/mm² (HI = 22 J/mm)

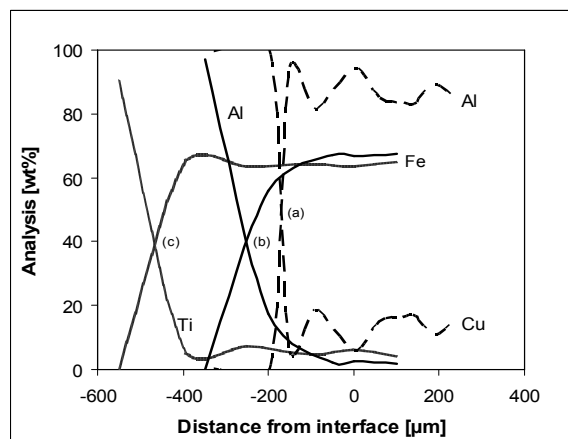


Figure 7: Variation in analysis across the fusion line for the a) Al/Cu, b) SS/Al and c) SS/Ti welds of the above samples

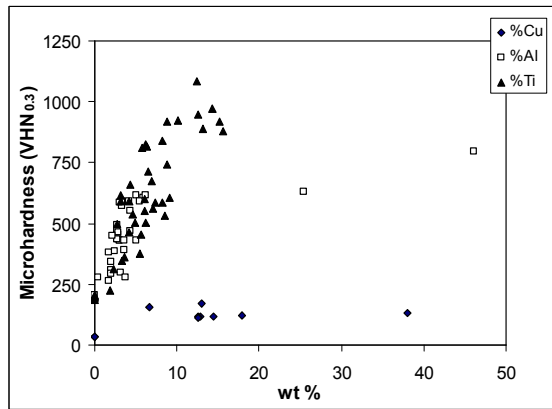


Figure 8: Microhardness within the weld as a function of the correspondent variation in main chemical components

The EDX analyses were correlated with the hardness obtained in those specific areas and are plotted in Figure 8. It can be seen that the hardness of the dissimilar welds increases with increasing content of Cu, Al and Ti within the three dissimilar metal combination welds respectively, with Ti having the greatest effect.

Tensile Shear Testing

The possible operating windows for the dissimilar metal combinations were determined for all three spot sizes and tensile shear testing was done on welds within these windows. The results are shown in Figures 9 - 11.

The parameter sets which yielded the highest tensile shear strengths for every spot size, were then further investigated (for Al/Cu and SS/Al) by means of varying the power, while keeping the travel speed constant, until the limits were again reached. Tensile shear testing was then also done on these welds and the results are also shown in Figures 9 - 10.

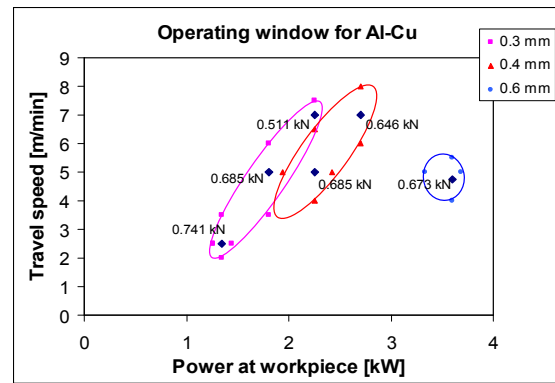
Al-Cu The possible operating windows for the specific set-up ranges approximately between 1.2 kW and 3.7 kW at travel speeds between 2 - 8 m/min. The least practical operating window would be for the 0.6 mm spot size.

The higher tensile shear strengths were obtained at the lower power levels and travel speeds. The highest tensile shear strength, with the least scatter, was obtained with power densities between 17 and 26 kW/mm², although the overall variation in tensile shear is not that much.

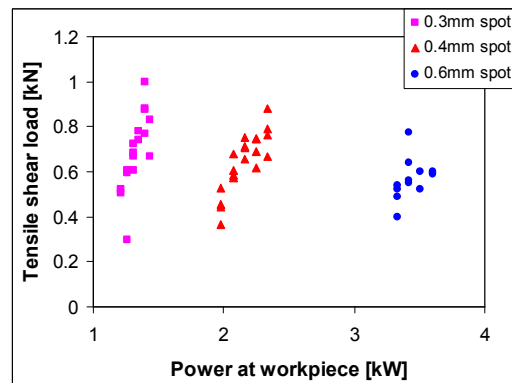
A 7 - 15% variation in power, at constant travel speed, resulted in a 35 - 50% variation in tensile shear strength for the different spot sizes. The increase in tensile shear strength with increasing power might be attributed to the corresponding increase in penetration and lengthening of fusion line.

From Fig 9b it is evident that the 0.3mm spot size delivered joints with higher tensile shear values, but in terms of the possible laser power variation, it had the smallest operating window. The 0.4mm spot size had the largest operating window (widest range in laser power variation) and second highest tensile shear values. Therefore, the 0.4mm spot size is the optimum for Al/Cu welding.

The fracture path of some of the tensile shear samples was through the weld itself, but mostly along the fusion line (decohesion mode).



a)



b)

Figure 9: a) Operating windows for Al/Cu at the different spot sizes and b) Variation in tensile shear strength with power (within operating window), at constant travel speed

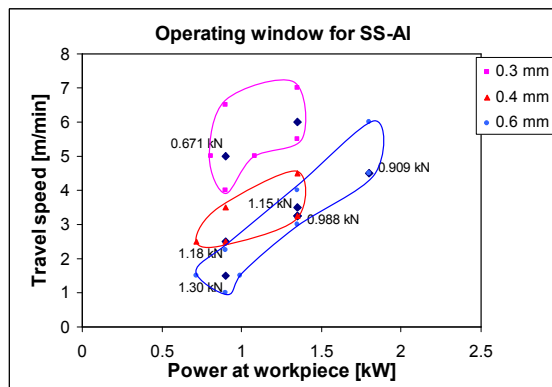
SS-Al The possible operating windows for the specific set-up ranges between 0.75 kW and 1.8 kW and 1 – 7 m/min.

Although some scatter was observed with the tensile shear strength values, the highest tensile shear strength is obtained at the lower power densities (higher heat inputs).

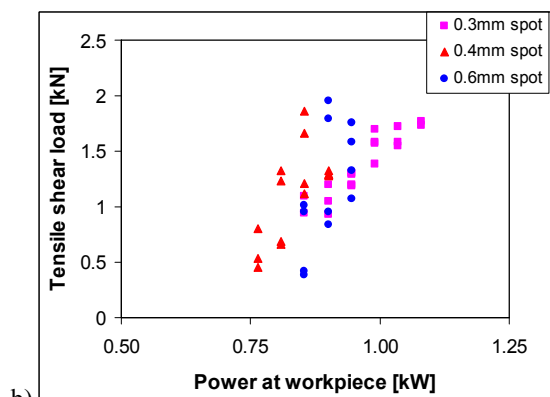
A 10 – 20% increase in welding power, at constant travel speed, resulted in a 40 – 65% increase in tensile shear strength for the different spot sizes.

Fig. 10b shows a large scatter in tensile shear values, and similar values, for the 0.4 and 0.6 mm spot sizes. Little scatter was obtained for the 0.3 mm spot, which is therefore the optimum for SS/Al welding.

The fracture path of some of the tensile shear specimens was through the weld itself, but mostly along the fusion line (decohesion mode). Some of the samples also showed shearing of the weld into the Al.



a)



b)

Figure 10: a) Operating windows for SS/Al at the different spot sizes and b) Variation in tensile shear strength with power (within operating window), at constant travel speed

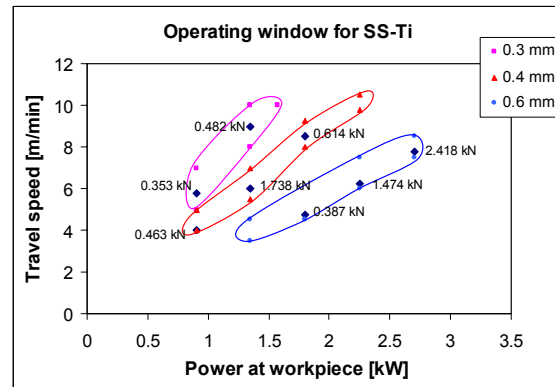


Figure 11: Operating windows for SS/Ti at the different spot sizes

SS-Ti The possible operating windows for the specific set-up ranges between 0.75 kW and 2.75 kW and 3.5 – 10 m/min.

With the exception of the 0.4mm spot size, the tensile shear strength of the lap welds increased with increasing welding speed, laser power and power density. For the 0.4mm spot, the tensile shear strength reached a maximum at 6 m/min and 1.35 kW and then decreased at higher speed and power. It can, therefore, be stated that there is a linear dependence of tensile shear strength on travel speed, power and power density for 0.3 and 0.6mm spot sizes. For the 0.4 mm spot however, a parabolic relationship was observed. The latter result was based on a single sample and should be verified.

As it is, the highest tensile shear strength was obtained at a power density between 8 and 11kW/mm² (13 and 22 J/mm) and from Fig. 11 it seems like the 0.6 mm spot size is the optimum for SS/Ti welding, but it would have to be verified.

The fracture path of all the tensile shear samples was along the fusion line (decohesion mode) and all the welds were extremely brittle. Therefore, most of the defect free joints, fractured during the subsequent preparation of samples for microstructural investigation.

Penetration characteristics

From Figure 12 it is evident that the tensile shear strength of the SS/Ti joints are dependant on the penetration characteristics of the welds. This can be attributed to the fracture path of all the samples, which were along the fusion line. The shear strength of the Al/Cu and SS/Al joints does, however, not show a total dependency on the dilution characteristics. This might be attributed to the fact

that not all the samples failed along the fusion line. Some samples failed in the weld metal and some showed shearing of the weld metal into the base metal.

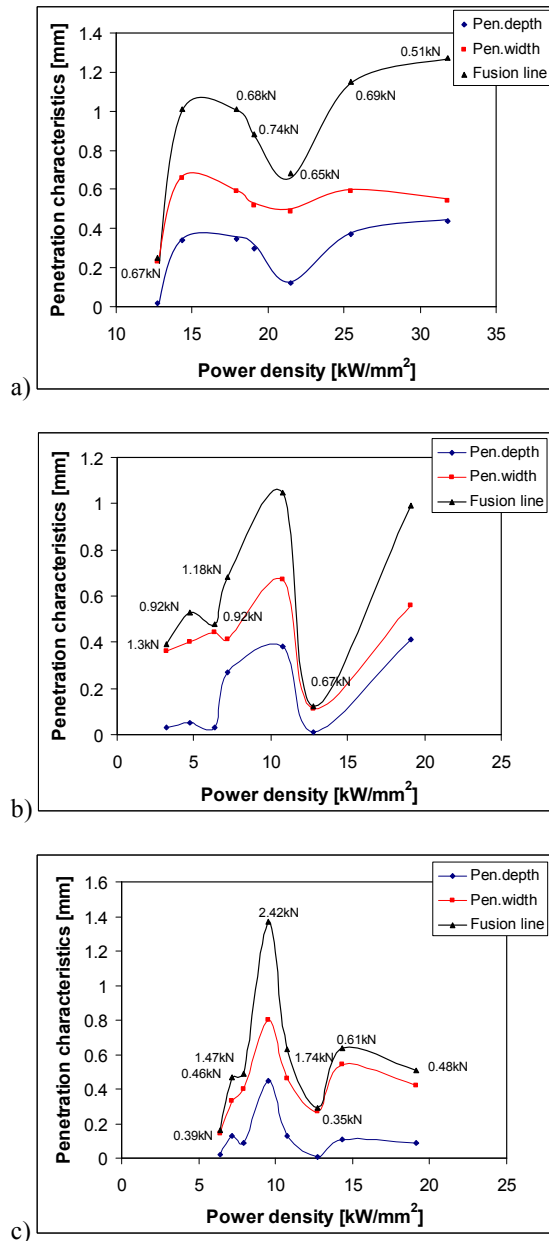


Figure 12: Dilution of the lap welds over the power density ranges investigated for a) Al/Cu, b) SS/Al and c) SS/Ti, coupled to the obtained tensile shear strength

General Insufficient clamping, resulting in small contact areas, lead to some poor joints being obtained, which might have otherwise resulted in good joints.

Linear relationships exist between power and travel speed required for welding of all three dissimilar metal combinations at all three spot sizes.

Conclusions

- The 0.4mm spot size had the largest operating window (widest range in laser power variation) and second highest tensile shear values. Therefore, the 0.4mm spot size is the optimum for Al/Cu welding.
- The 0.3 mm spot size delivered the optimum joint properties for SS/Al welding.
- It seems like the 0.6 mm spot size is the optimum for SS/Ti welding, but it would have to be verified.
- The SS/Ti welds were extremely hard and can be linked to the high tensile shear values. These joints were, however, also very brittle and are not functional.
- Narrow processing windows exist between sufficient fusion and excessive penetration, excessive spatter and weld stability for all three dissimilar metal combinations. Reproducibility was, therefore, also limited.
- By increasing the power (within the operating window) at a specific spot size and travel speed for Al/Cu and SS/Al, the tensile shear strength can be increased.
- The identification of the specific intermetallic phases present in the dissimilar metal welds were not in the scope of this investigation and will be included in future studies.

References

- [1] Joki, M. & Holtz, R. (2006) Experiences with laser beam welding of dissimilar materials, The Industrial Laser User 43, 26-29.
- [2] Mys, I. & Schmidt, M. (2006) Laser Micro Welding of Copper and Aluminum, in Proceedings of SPIE: Laser-based Micropackaging, CA, USA, 610703-1 – 610703-6.

[3] Van Tienhoven, J., Pathiraj, B. & Meijer, J. (2006) Laser joining of steel-aluminum joints in T-configuration, in Proceedings of 25th International Congress on Applications of Lasers and Electro-Optics (ICALEO), USA.

[4] Vollertsen, F. & Grupp, M. (2005) Laser beam joining of dissimilar thin sheet materials, Steel Research International, 76 No. 2/3, 240-244.

[5] Katayama, S. Usui, R. & Matsunawa, A. (1998) YAG Laser Welding of Steel to Aluminum, in Proceedings of the 5th International Conference on Trends in Welding Research, Pine Mountain, GA, 467-472.

[6] Mai, T.A. & Spowage, A.C. (2004) Characterisation of dissimilar joints in laser welding of steel-kovar, copper-steel and copper-aluminum, Materials Science and Engineering A374, 224 – 233.

[7] Sierra, G., Peyre, P., Deschaux-Beaume, F., Stuart, D. & Fras, G. (2007) Steel to aluminium key-hole laser welding, Materials Science and Engineering A447, 197-208.

[8] Joo, S-M., Kim, Y-P., Bang, H-S., Katayama, S. & Hwang, W-S. (2004) Welding of Steel and Aluminum by Nd-YAG Laser, Key Engineering Materials, Vols. 270-273, 2389-2394.

Meet the Authors

1. Maritha Theron holds a B.Eng(Met) degree. She has been involved in various fields of materials characterization (production processes and manufacturing) and was also part-time lecturer in Physical Metallurgy and Metallurgical Processes. She joined CSIR in 2006 and fields of interest include weld characterization and feasibility studies in Laser Welding (LMP).

2. Corney van Rooyen holds a masters degree in engineering and is certified by the International Institute of Welding as an international welding engineer. He has been involved in laser welding and cladding for the past six years. Fields of interest include martensitic stainless steel, Co and Ni-base alloys and light metals.

3. L.H. Ivanchev is a Senior Researcher at CSIR. Holds a PhD in Physical Metallurgy; BSc Mech Eng, and is a Univ Prof. in Physical Metallurgy and Metallurgical Processes of Technology. Particular expertise and interests include semi-solid metals technology, heat treatment and plastic deformation of metals. He is author and co-author of approx. 45 papers in technical journals and patent holder of three patents related semi-solid forming and heat treatment of metals.